

Rates and reversibilities in interconnected reaction networks

Ting C. Lin^a, Neil K. Razdan^a, and Aditya Bhan^{a, *}

^a*Department of Chemical Engineering and Materials Science, University of Minnesota-Twin Cities, 421 Washington Ave. SE, Minneapolis, Minnesota 55455, United States*

*Corresponding Author: E-mail: abhan@umn.edu; Fax: (+1) 612-626-7246

Keywords: reversibility, interconnected network, unidirectional rates, De Donder relation, isotopic tracing

Abstract

Mathematical relations prescribing unidirectional forward and reverse rates originally derived based on single-path reaction sequences do not apply to interconnected reaction networks. The presence of branches in reaction networks leading to alternative stable products decreases unidirectional rates in reference to those calculated by single-path functional forms as shown by simulated isotopic exchange rates, but impacts the unidirectional forward and reverse rates equally such that the functional form of effective reversibility remains unchanged. Regardless of stoichiometric numbers and network connectivity, application of the pseudo-steady-state hypothesis on reactive intermediates in conjunction with consideration of unidirectional rates toward the product of interest and all alternative stable products results in mathematical expressions that accurately reflect simulated isotopic exchange rates. Further analyses based on kinetic resistance, a property akin to electrical resistance, illustrate distinct contributions from elementary steps and nodal species to the unidirectional rates and kinetic resistances. The generalized formalism for assessing rates and reversibilities in interconnected networks derived herein enables us to demonstrate that unidirectional rates cannot be assessed solely from effective reversibilities and net rates of generation of stable species in such networks. However, isotopic exchange rates, under the condition that each elementary step in the overall reaction sequence forms a unique reactive intermediate that is consumed solely by the subsequent step, can be utilized to determine unidirectional rates and can serve to validate postulated reaction pathways in highly interconnected reaction networks (e.g., CO_x hydrogenation).

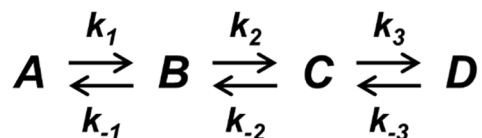
1 Introduction

1.1 Background

Kinetic descriptions of rates in reaction networks have emerged from a framework that considered single-path reaction sequences for simplicity of analysis[1–4]. This approach has served to establish base cases to consider for both research and pedagogical purposes. However, reaction networks with multiple end products, e.g., CO₂ hydrogenation to methanol occurring along with the reverse water-gas shift (RWGS) reaction[5–7] and formic acid decomposition following both a dehydrogenation and a dehydration pathway[8,9], are the norm. Reactor designs that employ polyfunctional formulations and other methods to couple reactions[10–13] further diverge from single-path systems and engender reaction networks with complex connectivity. This work thus aims to address the applicability of mathematical formalisms of rates and reversibility developed based on single-path reactions to interconnected reaction networks. We show here that the existence of branching pathways in reaction networks necessarily alters the functional forms of unidirectional rates while leaving the functional form of reversibility, along with any relations that stem from it, unchanged.

Rates and reversibility are two quantities ubiquitously used in the study of reaction kinetics, with the former further categorized into *net* rate and *unidirectional* rates. Net rate, defined as the difference between the unidirectional forward and reverse rates, and equal to the overall rate of change of species concentrations within a reactor, is more commonly reported. Unidirectional forward and reverse rates refer instead to the instantaneous rate of generation of products that corresponds to an equal consumption of reactants, and vice versa. An alternative interpretation of the unidirectional forward rate would be the *total* (as opposed to *net*) number of reactant molecules ($\Delta N_{\text{reactant}}$) that are transformed into a specific product species over a differential clock time (Δt)

or contact time ($\Delta\tau$) interval. The requirement to track the sources and sinks of molecules for directly measuring unidirectional rates necessitates the use of labeled species; this is accomplished experimentally with isotopically-labeled reactants and products under differential or near equilibrium reaction conditions and equating isotopic exchange rates with unidirectional rates[1,14,15]. The ratio of the unidirectional reverse rate to the unidirectional forward rate is then defined as the reversibility of the reaction such that reversibility adopts the value of unity when the unidirectional reverse and forward rates are equal (reaction is at equilibrium) and the value of zero when the unidirectional reverse rate is zero (reaction is unidirectionally forward). These descriptions of rates are defined for both an *elementary step* and an *overall reaction* consisting of multiple elementary steps. Throughout this work, we will notate the i^{th} elementary step net rate, unidirectional forward and reverse rates, and reversibility as r_i , \vec{r}_i , \tilde{r}_i , and z_i . An overall reaction from species I to species J then can be prescribed effective rates and reversibility (R_{IJ} , \vec{R}_{IJ} , \tilde{R}_{IJ} , and $Z_{\text{eff},IJ}$) that are analogous to a single-step event.



Scheme 1. Model single-path reaction system for the formation of species D from A with two reactive intermediates, species B and C, that abide by the pseudo-steady-state assumption.

Functional forms of unidirectional forward and reverse rates of a single-path reaction (e.g., Eqs. 1 & 2 for the system in Scheme 1) have been established by both Horiuti[1] and Temkin[16–18]. Here, the unidirectional forward rate is the rate at which the consumption of A leads to the formation of D while the unidirectional reverse rate is the rate at which the consumption of D leads to the formation of A.

$$\vec{R}_{AD,\text{single-path}} = \frac{\vec{r}_1 \vec{r}_2 \vec{r}_3}{\vec{r}_2 \vec{r}_3 + \tilde{r}_1 \vec{r}_3 + \tilde{r}_1 \tilde{r}_2} \quad (1)$$

$$\tilde{R}_{AD,\text{single-path}} = \frac{\tilde{r}_1 \tilde{r}_2 \tilde{r}_3}{\vec{r}_2 \vec{r}_3 + \tilde{r}_1 \vec{r}_3 + \tilde{r}_1 \tilde{r}_2} \quad (2)$$

Division of the unidirectional reverse rate by the unidirectional forward rate then yields the canonical functional form of the effective reversibility of the overall reaction (Eq. 3). This result, when combined with the De Donder relation (Eq. 4), further forms the basis for the generalized De Donder relation (Eq. 5), where A_i is the chemical affinity of the i^{th} elementary step[17,19].

$$Z_{\text{eff},AD} = \frac{\tilde{R}_{AD,\text{single-path}}}{\vec{R}_{AD,\text{single-path}}} = \frac{\tilde{r}_1 \tilde{r}_2 \tilde{r}_3}{\vec{r}_1 \vec{r}_2 \vec{r}_3} = \prod_i^3 z_i \quad (3)$$

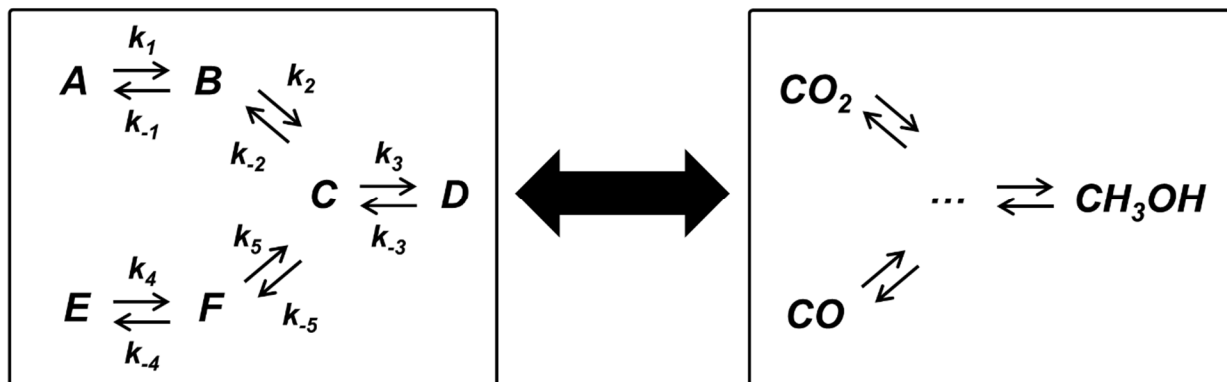
$$z_i = \frac{\tilde{r}_i}{\vec{r}_i} = \exp\left(-\frac{A_i}{RT}\right) \quad (4)$$

$$Z_{\text{eff},IJ} = \prod_i z_i = \exp\left(-\frac{\sum_i A_i}{RT}\right) \quad (5)$$

Application of Equations 1 to 3 on an interconnected reaction network with an additional branch (Scheme 2), however, demonstrates the inability for single-path unidirectional rate expressions to capture simulated isotopic exchange rates within an idealized plug-flow reactor (PFR) while the canonical expression of effective reversibility remains valid (Figs. 1 & 2). These behaviors of rates and reversibility reflect the dichotomous nature of kinetic and thermodynamic properties.

We provide, in this work, two generalized methods to obtain functional forms of unidirectional forward and reverse rates for any reaction network. The first relies on the concept of pseudo-steady-state hypothesis (PSSH) and mirrors the approach established by Horiuti[1] while the latter draws analogy with electrical circuits through the concept of kinetic resistance[20]. Regardless of the methodology, the result is consistent with the *dependence* of unidirectional rate expressions and the *independence* of the effective reversibility expression on network connectivity. In the following sections, we provide additional background on the principle of Horiuti's

derivation of unidirectional rates[1] and detail the isotopic exchange rate simulation we adopt to verify our derivations.



Scheme 2. Model system (left) for an interconnected network with stable species A, D, and E sharing a common reactive intermediate, species C. This system is analogous to CO_x hydrogenation where CO_2 , CO, and CH_3OH are interconnected (right; shown without stoichiometric amounts of H_2 and H_2O for simplicity).

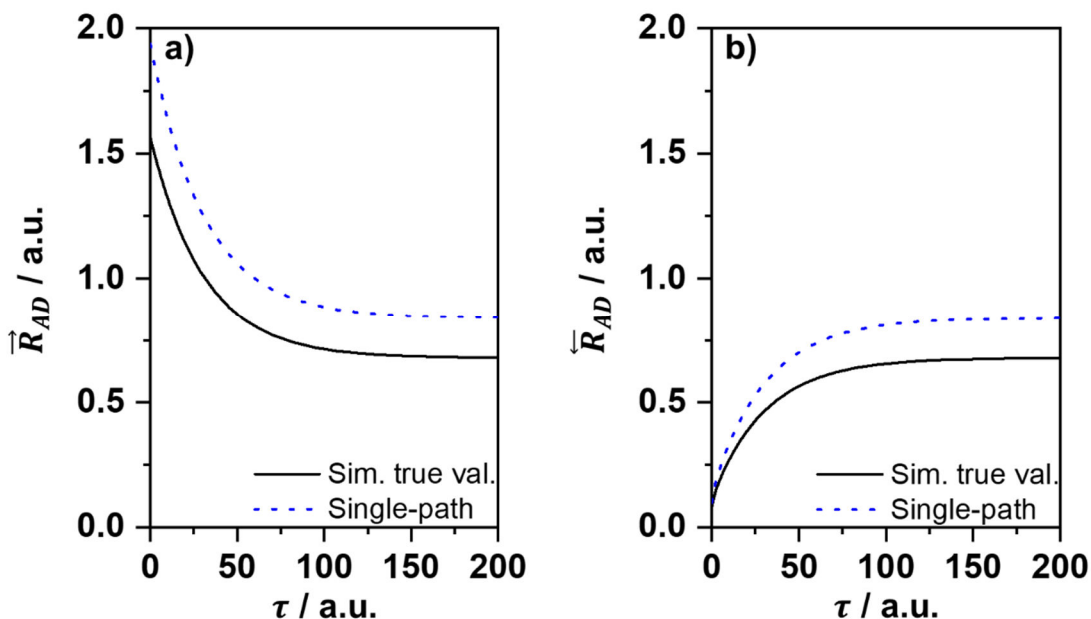


Figure 1. Unidirectional (a) forward and (b) reverse rates from species A to D as a function of contact time within an idealized PFR where the reaction network shown in Scheme 2 is occurring with the rate constants listed in Table 1. The black lines indicate simulated true values and the blue-dotted lines indicate values calculated based on Equations 1 and 2 (single-path system).

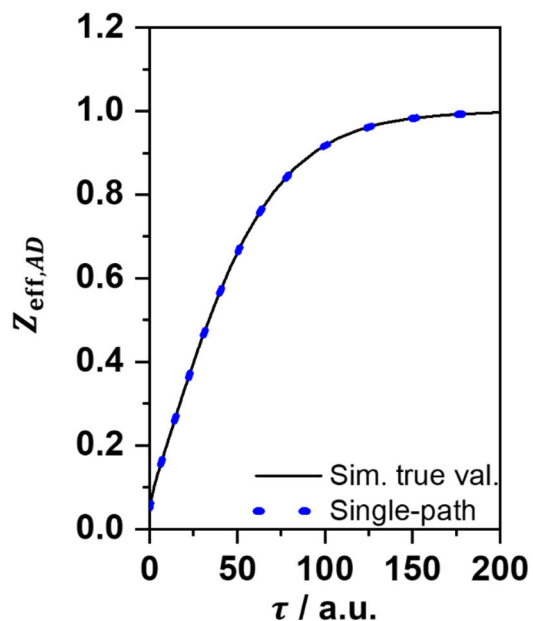


Figure 2. Effective reversibility of the reaction between species A to D as a function of contact time within an idealized PFR where the reaction network shown in Scheme 2 is occurring with the rate constants listed in Table 1. The black line indicates simulated true values and the blue-dotted line indicates values calculated based on Equation 3.

1.2 Horiuti's derivation of unidirectional rates for a single-path reaction

We consider here the model system shown in Scheme 1, wherein species A forms D following a single-path reaction mechanism with species B and C as the reactive intermediates. Here, the overall unidirectional forward rate may equivalently be defined as the rate of a cascade of events: i) A converts to B, ii) B converts to C, and iii) C converts to D. The unidirectional forward rate of the first event is simply \vec{r}_1 . To account for possible destinations of species B, we rely on the validity of PSSH on species B and C and note that the generated B from the first step must either reform reactant A or continue down the pathway to generate species D. This enables us to express the unidirectional forward rate from A to D as the product between the first elementary step and a probability factor that captures the fraction of B that will lead to species D (Eq. 6)[1].

$$\vec{R}_{AD} = \vec{r}_1 \left(\frac{\vec{R}_{BD}}{\vec{r}_1 + \vec{R}_{BD}} \right) \quad (6)$$

This procedure reduces the system to the reaction from B to D, for which we can construct Equation 7 following the same argument.

$$\vec{R}_{BD} = \vec{r}_2 \left(\frac{\vec{R}_{CD}}{\vec{r}_2 + \vec{R}_{CD}} \right) \quad (7)$$

The system is then reduced to a single elementary step, enabling a simple substitution using Equation 8.

$$\vec{R}_{CD} = \vec{r}_3 \quad (8)$$

Algebraic manipulations along with a completely analogous consideration of $\vec{R}_{AD} = \vec{R}_{DA}$ result in Equations 1 and 2 for the single-path unidirectional forward and reverse rates from A to D, which are the same expressions as those derived using Temkin's product rule[16–18] (Derivation in Sec. S1 & S2; Supporting Information (SI)). Note that while we have summarized the derivation here for a single-path reaction with only three elementary steps, the method holds for single-path reactions of arbitrary length. In this work, we will expand upon Horiuti's methodology as it is readily generalizable to interconnected reaction systems.

1.3 Model system to consider and simulation methodology

We illustrate the behaviors of unidirectional rates and effectivity reversibility in interconnected reaction networks by simulating the system shown in Scheme 2 with the rate constants listed in Table 1 and the initial conditions of $C_{A,0} = 100$ a.u. and $C_{D,0} = C_{E,0} = 2$ a.u. This reaction system reflects a simplified network where three stable species (A, D, and E) may each react to yield another stable species through a common reactive intermediate; such a reaction network is analogous to processes such as methanol synthesis from syngas mixtures, where both CO_2 and/or CO may hydrogenate to form methanol with CO_2 and CO further related via the RWGS

reaction[5–7]. We will focus primarily on the unidirectional forward and reverse rates and the effective reversibility between species A and D, which, for the CO₂/CO/CH₃OH system, would by analogy inform us on the unidirectional forward and reverse rates and the effective reversibility of the CO₂ hydrogenation to methanol pathway, free of convolution from CO hydrogenation and RWGS pathways. Other relationships may be derived following the same approach with the unidirectional forward and reverse rates and the effective reversibility between species A and E provided in Section S3 (SI).

Table 1. Rate constants used to simulate the concentration profiles, unidirectional rates, and effective reversibility within an idealized PFR where the interconnected reaction network shown in Scheme 2 is occurring.

Elementary step	1	2	3	4	5
k_i / a.u.	3	0.2	20	10	1
k_{-i} / a.u.	30	0.5	2	50	5

The validity of mathematically-derived functional forms of unidirectional rates will be established based on comparisons of calculated unidirectional rates with simulated isotopic exchange rates within an idealized PFR where PSSH is strictly adhered to by all reactive intermediates (species B, C, and F in Scheme 2). MATLAB computational code for the simulation is provided in Section S4 (SI) and verified with single-path formalisms (Eqs. 1 & 2) (Sec. S5; Fig. S3; SI), but the procedure is illustrated in Figure 3 and summarized as:

- (i) simulate concentration profiles for all species over contact time in an idealized PFR,
- (ii) at each contact time, convert the reactant of interest into its isotopically-labeled form denoted with a prime (e.g., for the unidirectional forward rate of A to D, all A will be converted to A' at each instance in contact time), and

- (iii) re-simulate the instantaneous rate of generation of isotopically-labeled product with the concentrations and isotopic fractions of reactive intermediates governed by PSSH. This simulated rate is equivalent to the isotopic exchange rate and the unidirectional rate (e.g., the rate of generation of D' is the isotopic exchange rate and the unidirectional forward rate from A to D).

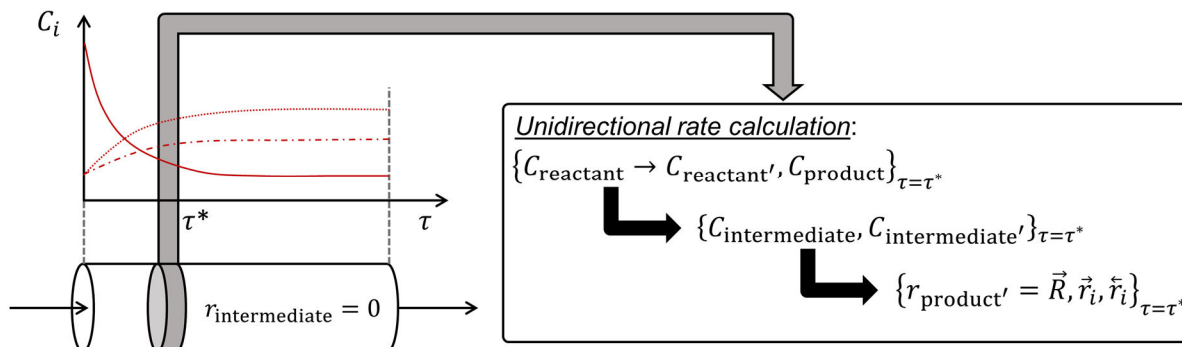


Figure 3. A schematic illustration for the calculation of simulated unidirectional rates based on the isotopic exchange rate at every instance in τ along an idealized PFR.

2 Results and Discussion

2.1 PSSH viewpoint for the derivation of unidirectional rates

2.1.1 Unidirectional forward rate from A to D

We are here interested in determining the functional form of the unidirectional forward rate from species A to D (\vec{R}_{AD}) shown in Scheme 2 in terms of the unidirectional rates of elementary steps (\vec{r}_k and \hat{r}_k , for $k \in [1, 5]$). The underlying principle outlined by Horiuti is correct, but generalization of the derivation to an interconnected reaction network necessitates accounting of alternative pathways within the probability factor, which can be visualized and made apparent by reorganizing the reaction network shown in Scheme 2 to one that explicitly portrays the unidirectional conversion of species A to all other stable species going from left to right (Fig. 4). Note that the directions of elementary steps 4 and 5 in Figure 4 are reversed relative to Scheme 2

due to the rearrangement of species. We adopt the “land post” symbol in Horiuti’s work[1], where each vertical post indicates an intermediate state that every A molecule must pass through prior to reaching the final product state. The red-dashed land post signifies the presence of a nodal species where the reaction path branches.

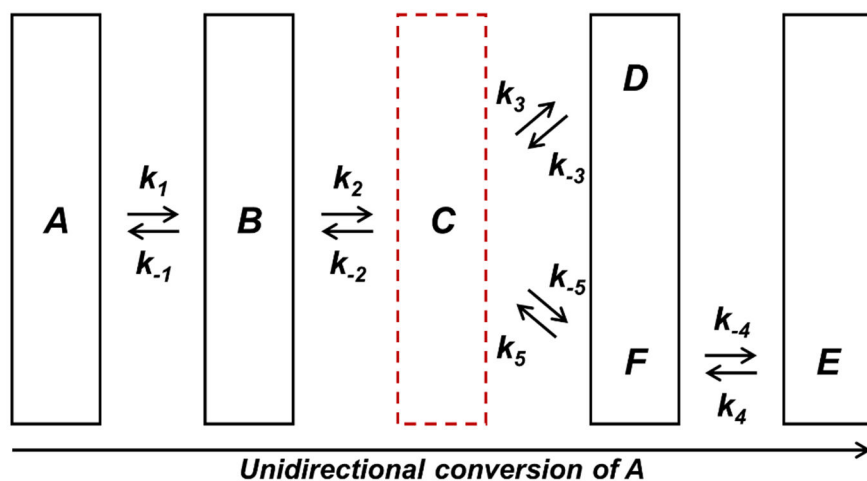


Figure 4. Rearrangement and land post assignment of the interconnected system shown in Scheme 2 for the unidirectional conversion of species A to species D and E. The red-dashed land post signifies the nodal species after which the reaction network branches.

Under the validity of PSSH for B, the unidirectional forward rate from A to D remains unchanged as the product between the unidirectional forward rate of the first elementary step (generation of B) and the probability that species B cascades to generate species D (consumption of B to form exclusively D) (Eq. 9).

$$\vec{R}_{AD} = \vec{r}_1 \left(\frac{\vec{R}_{BD}}{\vec{r}_1 + \vec{R}_{BD} + \vec{R}_{BE}} \right) \quad (9)$$

It then becomes apparent that the unidirectional forward rate of an interconnected reaction system inherently differs from that of a single-path reaction system and the former inevitably depends on rates of the additional branch (elementary steps 4 and 5 in this case), which is accounted for by the extra term in the denominator (\vec{R}_{BE} in this case). The existence of the alternative stable product, E, also impacts the unidirectional forward rate from B to D and from B to E,

$$\vec{R}_{BD} = \vec{r}_2 \left(\frac{\vec{R}_{CD}}{\vec{r}_2 + \vec{R}_{CD} + \vec{R}_{CE}} \right) \quad (10)$$

$$\vec{R}_{BE} = \vec{r}_2 \left(\frac{\vec{R}_{CE}}{\vec{r}_2 + \vec{R}_{CD} + \vec{R}_{CE}} \right) \quad (11)$$

and only ceases to be sensed by the system after the nodal species (species C; red-dashed land post; Fig. 4). All steps after the nodal species and nodal land post are not impacted by alternative branches as those pathways are no longer viable end points after we have crossed the nodal land post. Thus, Equations 12-14 outline the remaining required unidirectional forward rate expressions.

$$\vec{R}_{CD} = \vec{r}_3 \quad (12)$$

$$\vec{R}_{CE} = \vec{r}_5 \left(\frac{\vec{R}_{FE}}{\vec{r}_5 + \vec{R}_{FE}} \right) \quad (13)$$

$$\vec{R}_{FE} = \vec{r}_4 \quad (14)$$

Algebraic manipulations of Equations 9 to 14 (detailed in Sec. S6; SI) yield the functional form of the unidirectional forward rate from A to D in terms of only the elementary step unidirectional rates within the reaction network (Eq. 15).

$$\vec{R}_{AD} = \frac{\vec{r}_1 \vec{r}_2 \vec{r}_3}{\vec{r}_2 \vec{r}_3 + \vec{r}_1 \vec{r}_3 + \vec{r}_1 \vec{r}_2 + (\vec{r}_1 + \vec{r}_2) \left(\frac{\vec{r}_4 \vec{r}_5}{\vec{r}_4 + \vec{r}_5} \right)} \quad (15)$$

Equation 15 now explicitly shows that \vec{R}_{AD} is indeed dependent on the rates of elementary steps 4 and 5, an expected result affirming that the presence of alternative pathways impacts the rates of reaction. Calculated values of unidirectional forward rate based on Equation 15 is also in full accord with the simulated isotopic exchange rates at all contact times within an idealized PFR (Fig. 5). We next investigate the impact of elementary steps 4 and 5 on the unidirectional reverse rate from species A to D and reserve the physical interpretation of the functional forms of unidirectional rates for Section 2.2.

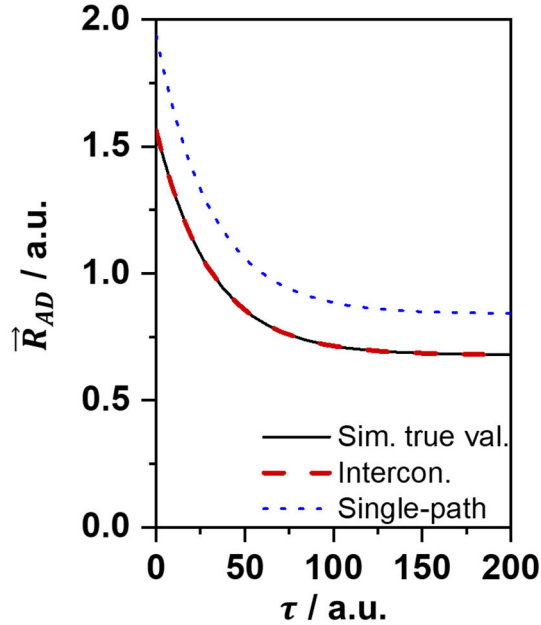


Figure 5. Unidirectional forward rate from species A to D as a function of contact time within an idealized PFR where the reaction network shown in Scheme 2 is occurring with the rate constants listed in Table 1. The black line indicates simulated true values, the red-dashed line indicates values calculated based on Equation 15 (single-node system), and the blue-dotted line indicates values calculated based on Equation 1 (single-path system).

2.1.2 Unidirectional reverse rate from A to D

We now derive the functional form of the unidirectional reverse rate from species A to D (\tilde{R}_{AD}) shown in Scheme 2 in terms of the unidirectional rates of elementary steps (\vec{r}_k and \tilde{r}_k , for $k \in [1, 5]$) by instead considering the unidirectional forward rate from species D to A (\vec{R}_{DA}); the two quantities are equivalent and doing so allows us to adopt the exact same methodology as that applied for the unidirectional forward rate from A to D. Again, the reaction network shown in Scheme 2 can be first rearranged into one that reflects the unidirectional conversion of species D to all other stable species from left to right to facilitate visualization of the appropriate probability factors (Fig. 6).

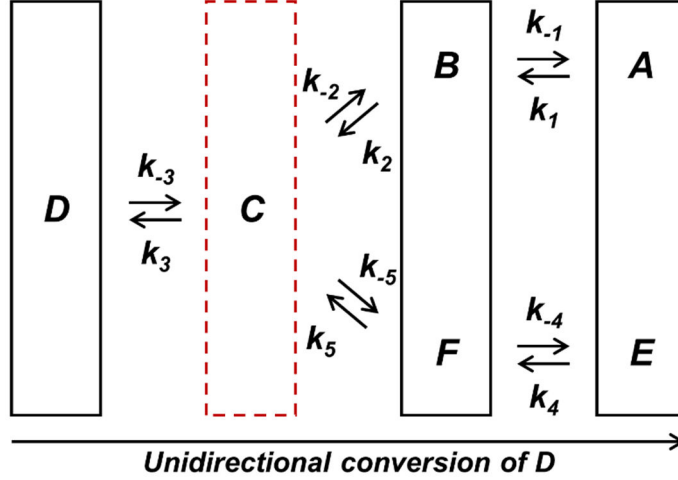


Figure 6. Rearrangement and land post assignment of the interconnected system shown in Scheme 2 for the unidirectional conversion of species D to species A and E. The red-dashed land post signifies the nodal species after which the reaction network branches.

The unidirectional rate expressions necessary for the derivation of \vec{R}_{DA} are outlined in Equations 16 to 20. In contrast with the analysis for \vec{R}_{AD} , the nodal land post, illustrated by the red-dashed land post, is now the second step as opposed to the third step (Fig. 6). This property indicates that the effect of having a branch in reaction pathway will only impact the first probability factor (Eq. 16) while all later steps remain unaffected (Eqs. 17-20) in reference to the rates of a single-path reaction sequence.

$$\vec{R}_{AD} = \vec{R}_{DA} = \tilde{r}_3 \left(\frac{\vec{R}_{CA}}{\tilde{r}_3 + \vec{R}_{CA} + \vec{R}_{CE}} \right) \quad (16)$$

$$\vec{R}_{CA} = \tilde{r}_2 \left(\frac{\vec{R}_{BA}}{\tilde{r}_2 + \vec{R}_{BA}} \right) \quad (17)$$

$$\vec{R}_{BA} = \tilde{r}_1 \quad (18)$$

$$\vec{R}_{CE} = \tilde{r}_5 \left(\frac{\vec{R}_{FE}}{\tilde{r}_5 + \vec{R}_{FE}} \right) \quad (19)$$

$$\vec{R}_{FE} = \tilde{r}_4 \quad (20)$$

With algebraic manipulations of Equations 16 to 20 (detailed in Sec. S7; SI), \vec{R}_{AD} may be expressed strictly in terms of the elementary step unidirectional rates within the reaction network (Eq. 21). The result again explicitly shows the involvement of unidirectional rates of elementary steps 4 and 5 in the expression for the unidirectional reverse rate from A to D and reflect the simulated isotopic exchange rates (Fig. 7).

$$\vec{R}_{AD} = \frac{\vec{r}_1 \vec{r}_2 \vec{r}_3}{\vec{r}_2 \vec{r}_3 + \vec{r}_1 \vec{r}_3 + \vec{r}_1 \vec{r}_2 + (\vec{r}_1 + \vec{r}_2) \left(\frac{\vec{r}_4 \vec{r}_5}{\vec{r}_4 + \vec{r}_5} \right)} \quad (21)$$

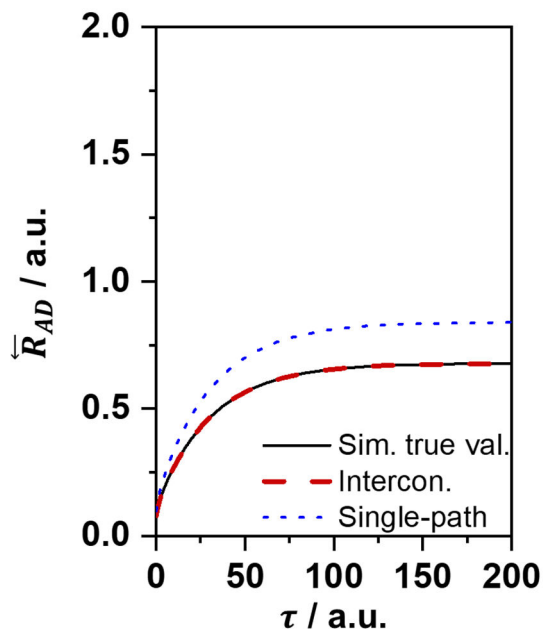


Figure 7. Unidirectional reverse rate from species A to D as a function of contact time within an idealized PFR where the reaction network shown in Scheme 2 is occurring with the rate constants listed in Table 1. The black line indicates simulated true values, the red-dashed line indicates values calculated based on Equation 21 (single-node system), and the blue-dotted line indicates values calculated based on Equation 2 (single-path system).

2.1.3 Effective reversibility from A to D

The resulting expressions of \vec{R}_{AD} and \vec{R}_{AD} outlined in Sections 2.1.1 and 2.1.2 are specifically for the system depicted in Scheme 2. Despite of the connectivity-*dependent* nature of

unidirectional rates, division of \vec{R}_{AD} by \vec{R}_{AD} again yields the canonical functional form of effective reversibility (Eq. 22).

$$Z_{\text{eff},AD} = \frac{\vec{R}_{AD}}{\vec{R}_{AD}} = \frac{\tilde{r}_1 \tilde{r}_2 \tilde{r}_3}{\vec{r}_1 \vec{r}_2 \vec{r}_3} = \prod_i^3 z_i \quad (22)$$

This is consistent with the observation illustrated in Figure 2 and demonstrates the connectivity-*independent* nature of effective reversibility as the functional form of effective reversibility is unchanged between a single-path system (Scheme 1) and a single-node system (Scheme 2). In other words, the effective reversibility between stable species within any interconnected reaction network is equal to the product of the reversibilities of the elementary steps that connect them. Any alternative pathways (steps 4 and 5 in this case) do not appear in the functional form of the effective reversibility. Next, we provide an alternative interpretation of Equations 15 and 21 that facilitates formulation of unidirectional rates of higher order reaction networks with multiple nodal species.

2.2 Physical interpretation with the kinetic resistance viewpoint

The derivation thus far represents a *PSSH* viewpoint, with Equations 15 and 21 largely justified by algebra alone. To understand the resulting expressions, we adopt a *kinetic resistance* viewpoint by drawing analogy between the inverse of unidirectional rate and resistance in electrical circuits. Such an analogy has been previously adopted in the study of reaction route graphs[20]. Here, we will focus on investigating the forward kinetic resistance, defined as the kinetic resistance associated with the unidirectional forward rate, and note that the reverse kinetic resistance behaves analogously (Sec. S8; SI). The inverse of the unidirectional forward rate from A to D for the single-path reaction system in Scheme 1 and Table 2 (Eq. 1) is the weighted sum of the inverse of unidirectional forward rates of the elementary steps involved (Eq. 23).

$$\frac{1}{\vec{R}_{AD,\text{single-path}}} = \frac{1}{\vec{r}_1} + \frac{z_1}{\vec{r}_2} + \frac{z_1 z_2}{\vec{r}_3} \quad (23)$$

This expression is equivalent to a series of resistors having an overall resistance that is the sum of their individual resistances (Table 2; row 1); $1/\vec{R}_{AD,\text{single-path}}$ is the forward kinetic resistance from A to D and $(\prod_{j=0}^{i-1} z_j)/\vec{r}_i$, where $z_0 = 1$, is the forward kinetic resistance of the i^{th} elementary step. As we progress down the reaction pathway, the influence of each elementary step is weighted by the reversibility of the previous steps, a consequence of the decrease in driving force experienced by the i^{th} step due to all preceding steps. A fully reversible ($z_i = 1$) elementary step therefore does not reduce the driving force experienced by the later steps. This behavior is congruent with the fact that if all elementary steps have the same reversibility, the later steps will necessarily be less rate controlling than the first elementary step[2,21]. Thus, the general form of the forward kinetic resistance for a single-path reaction from species A to P over N steps is given by Equation 24, which is also manifested in Horiuti's derivation[1] but was not interpreted.

$$\frac{1}{\vec{R}_{AP,\text{single-path}}} = \sum_{i=1}^N \frac{\prod_{j=0}^{i-1} z_j}{\vec{r}_i} \quad \text{where } z_0 = 1 \quad (24)$$

The unidirectional rates and kinetic resistances in an interconnected system may be analyzed in the same manner. Inverting the unidirectional forward rate from A to D in our model single-node system (Eq. 15; Scheme 2) demonstrates that the forward kinetic resistance from A to D is the sum of the forward kinetic resistance of the *single-path* reaction from A to D and a nodal resistance term associated with the nodal species, C, consisting of the forward kinetic resistance from species A up to the species C and the inverse of the branching ratio of species C leading to species D over species E (Eq. 25).

$$\frac{1}{\vec{R}_{AD}} = \frac{1}{\vec{r}_1} + \frac{z_1}{\vec{r}_2} + \frac{z_1 z_2}{\vec{r}_3} + \frac{1}{\vec{R}_{AC}} \left(\frac{\vec{R}_{CD}}{\vec{R}_{CE}} \right)^{-1} = \underbrace{\frac{1}{\vec{R}_{AD, \text{single-path}}}}_{\text{single-path forward kinetic resistance}} + \underbrace{\frac{1}{\vec{R}_{AC}} \left(\frac{\vec{R}_{CD}}{\vec{R}_{CE}} \right)^{-1}}_{\text{nodal forward kinetic resistance}} \quad (25)$$

The resistor diagram is similar to that for a single-path system except the nodal species is replaced by a nodal resistor (Table 2; row 2). Manifestation of nodal resistances in branching electrical circuits can also be shown (Sec. S9; SI). The analogous reverse kinetic resistance from A to D reveals that \vec{R}_{CE} is unchanged while all other terms will change direction and be associated with the unidirectional reverse rates (Eq. 26).

$$\frac{1}{\vec{R}_{AD}} = \frac{1}{\vec{R}_{AD, \text{single-path}}} + \frac{1}{\vec{R}_{AC}} \left(\frac{\vec{R}_{CD}}{\vec{R}_{CE}} \right)^{-1} \quad (26)$$

Since $\vec{R}_{AD, \text{single-path}}$, \vec{R}_{AC} , and \vec{R}_{CD} are each single-path unidirectional reverse rates, the direction may be reversed using the canonical definition of effective reversibility (Eq. 3).

$$\frac{1}{\vec{R}_{AD}} = \frac{1}{z_1 z_2 z_3 \vec{R}_{AD, \text{single-path}}} + \frac{1}{z_1 z_2 \vec{R}_{AC}} \left(\frac{z_3 \vec{R}_{CD}}{\vec{R}_{CE}} \right)^{-1} \quad (27)$$

Dividing the forward kinetic resistance from A to D (Eq. 25) by the reverse kinetic resistance from A to D (Eq. 27) then consistently proves that the effect of the alternative pathway (\vec{R}_{CE}) cancels out for the effective reversibility but not for unidirectional rates and kinetic resistances.

Derivations of unidirectional rates for the two-node systems shown in Table 2 illustrate that nodal resistances written in the same form as those in Equations 25 and 26 fully account for branching in the reaction network such that the branching ratios consist of single-path unidirectional rates toward the product of interest regardless of the number of nodal species (Table 2; derivations in Sec. S10 & S11; SI). Specifically, when evaluating the forward kinetic resistance from A to E for the two-node system shown in Table 2, the branching ratio in the nodal resistance

contributed by species C is just the ratio of the single-path unidirectional forward rate from C to E over the unidirectional forward rate from C to H (innately single-path). The existence of the alternative stable product F is captured by the second nodal resistance contributed by species D. In the case where the nodal species leads to more than one alternative products (e.g., species C in the evaluation of forward kinetic resistance from A to H in the two-node system in Table 2), the branching ratio will be the single-path unidirectional forward rate to the product of interest (H in this case) over the sum of unidirectional forward rates to all alternative products (E and F in this case) (Sec. S12; SI). Hence, the general form of the nodal resistance contributed by nodal species I for the forward kinetic resistance from species A to P with M alternative products ($P_{\text{alt},j}$) branching from I may be defined as

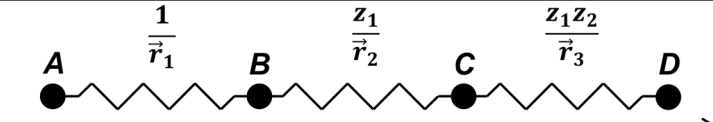
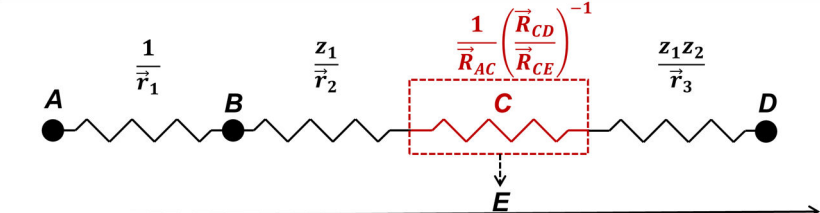
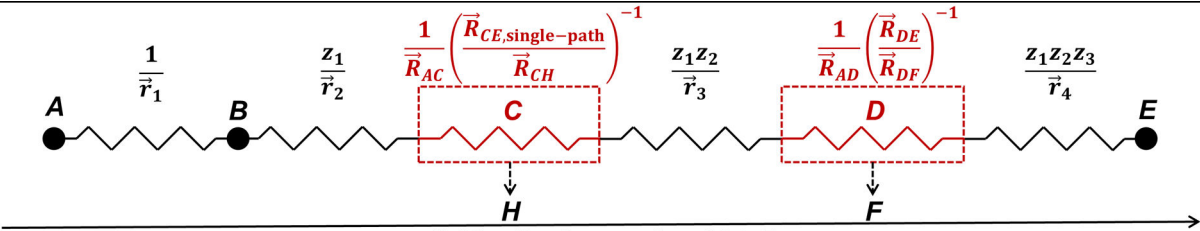
$$\text{forward nodal resistance of } I = \frac{1}{\vec{R}_{AI}} \left(\frac{\vec{R}_{IP, \text{single-path}}}{\sum_{j=1}^M \vec{R}_{IP_{\text{alt},j}}} \right)^{-1} \quad (28)$$

The kinetic resistance viewpoint therefore not only offers physical interpretation for the functional forms of unidirectional rates but also presents a direct method for the derivation of unidirectional rates in interconnected reaction networks:

- (i) write out the single-path kinetic resistance of the pathway of interest (Eq. 24),
- (ii) convert all nodal species to nodal resistances (Eq. 28), and
- (iii) invert the overall kinetic resistance (sum of (i) and (ii)).

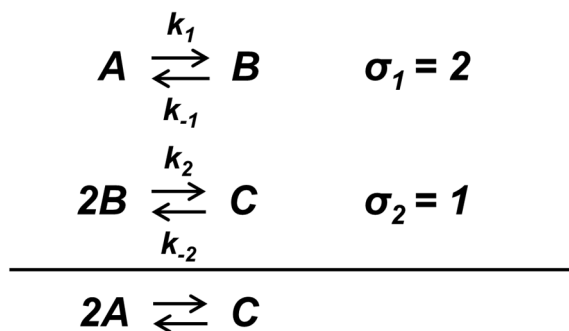
In the following section, we further generalize the formalism outlined thus far and consider reaction systems where the stoichiometric numbers of elementary steps are not unity.

Table 2. Resistor diagrams, forward kinetic resistances, and forward rates for single-path, single-node, and two-node systems.

Reaction mechanism	Resistor diagram, forward kinetic resistance, and forward rate
$A \xrightleftharpoons[k_{-1}]{k_1} B \xrightleftharpoons[k_{-2}]{k_2} C \xrightleftharpoons[k_{-3}]{k_3} D$ <p>Single-path</p>	 <p>Unidirectional conversion of A to D</p> $\frac{1}{\vec{R}_{AD}} = \frac{1}{\vec{r}_1} + \frac{z_1}{\vec{r}_2} + \frac{z_1 z_2}{\vec{r}_3}$ $\vec{R}_{AD} = \vec{r}_1 \vec{r}_2 \vec{r}_3 [\vec{r}_2 \vec{r}_3 + \vec{r}_1 \vec{r}_3 + \vec{r}_1 \vec{r}_2]^{-1}$
$A \xrightleftharpoons[k_{-1}]{k_1} B \xrightleftharpoons[k_{-2}]{k_2} C \xrightleftharpoons[k_{-3}]{k_3} D$ $E \xrightleftharpoons[k_{-4}]{k_4} F \xrightleftharpoons[k_{-5}]{k_5} C$ <p>Single-node</p>	 <p>Unidirectional conversion of A to D</p> $\frac{1}{\vec{R}_{AD}} = \frac{1}{\vec{r}_1} + \frac{z_1}{\vec{r}_2} + \frac{z_1 z_2}{\vec{r}_3} + \frac{1}{\vec{R}_{AC}} \left(\frac{\vec{R}_{CD}}{\vec{R}_{CE}} \right)^{-1}$ $\vec{R}_{AD} = \vec{r}_1 \vec{r}_2 \vec{r}_3 \left[\vec{r}_2 \vec{r}_3 + \vec{r}_1 \vec{r}_3 + \vec{r}_1 \vec{r}_2 + (\vec{r}_1 + \vec{r}_2) \left(\frac{\vec{r}_4 \vec{r}_5}{\vec{r}_4 + \vec{r}_5} \right) \right]^{-1}$
$A \xrightleftharpoons[k_{-1}]{k_1} B \xrightleftharpoons[k_{-2}]{k_2} C \xrightleftharpoons[k_{-3}]{k_3} D \xrightleftharpoons[k_{-4}]{k_4} E$ $C \xrightleftharpoons[k_{-5}]{k_5} F \xrightleftharpoons[k_{-6}]{k_6} G \xrightleftharpoons[k_{-7}]{k_7} H$ <p>Two-node</p>	 <p>Unidirectional conversion of A to E</p> $\frac{1}{\vec{R}_{AE}} = \frac{1}{\vec{r}_1} + \frac{z_1}{\vec{r}_2} + \frac{z_1 z_2}{\vec{r}_3} + \frac{z_1 z_2 z_3}{\vec{r}_4} + \frac{1}{\vec{R}_{AC}} \left(\frac{\vec{R}_{CE, \text{single-path}}}{\vec{R}_{CH}} \right)^{-1} + \frac{1}{\vec{R}_{AD}} \left(\frac{\vec{R}_{DE}}{\vec{R}_{DF}} \right)^{-1}$ $\vec{R}_{AE} = \vec{r}_1 \vec{r}_2 \vec{r}_3 \vec{r}_4 \left[\vec{r}_2 \vec{r}_3 \vec{r}_4 + \vec{r}_1 \vec{r}_3 \vec{r}_4 + \vec{r}_1 \vec{r}_2 \vec{r}_4 + \vec{r}_1 \vec{r}_2 \vec{r}_3 + \vec{r}_1 \vec{r}_2 \vec{r}_5 + \vec{r}_1 \vec{r}_3 \vec{r}_5 + \vec{r}_2 \vec{r}_3 \vec{r}_5 + (\vec{r}_1 + \vec{r}_2) (\vec{r}_3 + \vec{r}_4 + \vec{r}_5) \left(\frac{\vec{r}_6 \vec{r}_7}{\vec{r}_6 + \vec{r}_7} \right) \right]^{-1}$

2.3 Non-unity stoichiometric numbers

The presence of non-unity stoichiometric numbers (σ_i) in a single-path system has already been reconciled by Horiuti's formalism[1]. For the system shown in Scheme 3, where two elementary steps can occur with the first step having the stoichiometric number of two and the second step having unity stoichiometric number to yield the overall reaction $2A \rightleftharpoons C$, we can construct the land post diagram but note that the *apparent* unidirectional rates of the first step (\vec{r}'_1 , $\vec{r}'_1, 2A \rightleftharpoons 2B$) must be the unidirectional rates of the first elementary step divided by a factor of two (i.e., $\vec{r}'_1 = \vec{r}_1/2$ and $\tilde{r}'_1 = \tilde{r}_1/2$) to account for the non-unity stoichiometric number (Fig. 8). It then becomes evident that the procedure outlined in Section 1.2 remains valid as long as the apparent elementary step unidirectional rates for the first step are used instead.



Scheme 3. Example single-path reaction system for the formation of species C from 2A with one reactive intermediate, species B, that abide by the pseudo-steady-state assumption.

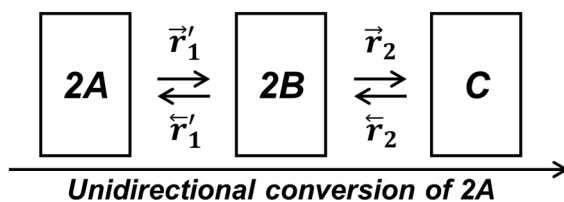


Figure 8. Land post assignment for the single-path system shown in Scheme 3 for the unidirectional conversion of 2A to C.

Non-unity stoichiometric numbers within an interconnected network can be taken into account similarly; however, it is the assignment of stoichiometric numbers that is less straightforward. We now consider a system with four unique elementary steps where two possible

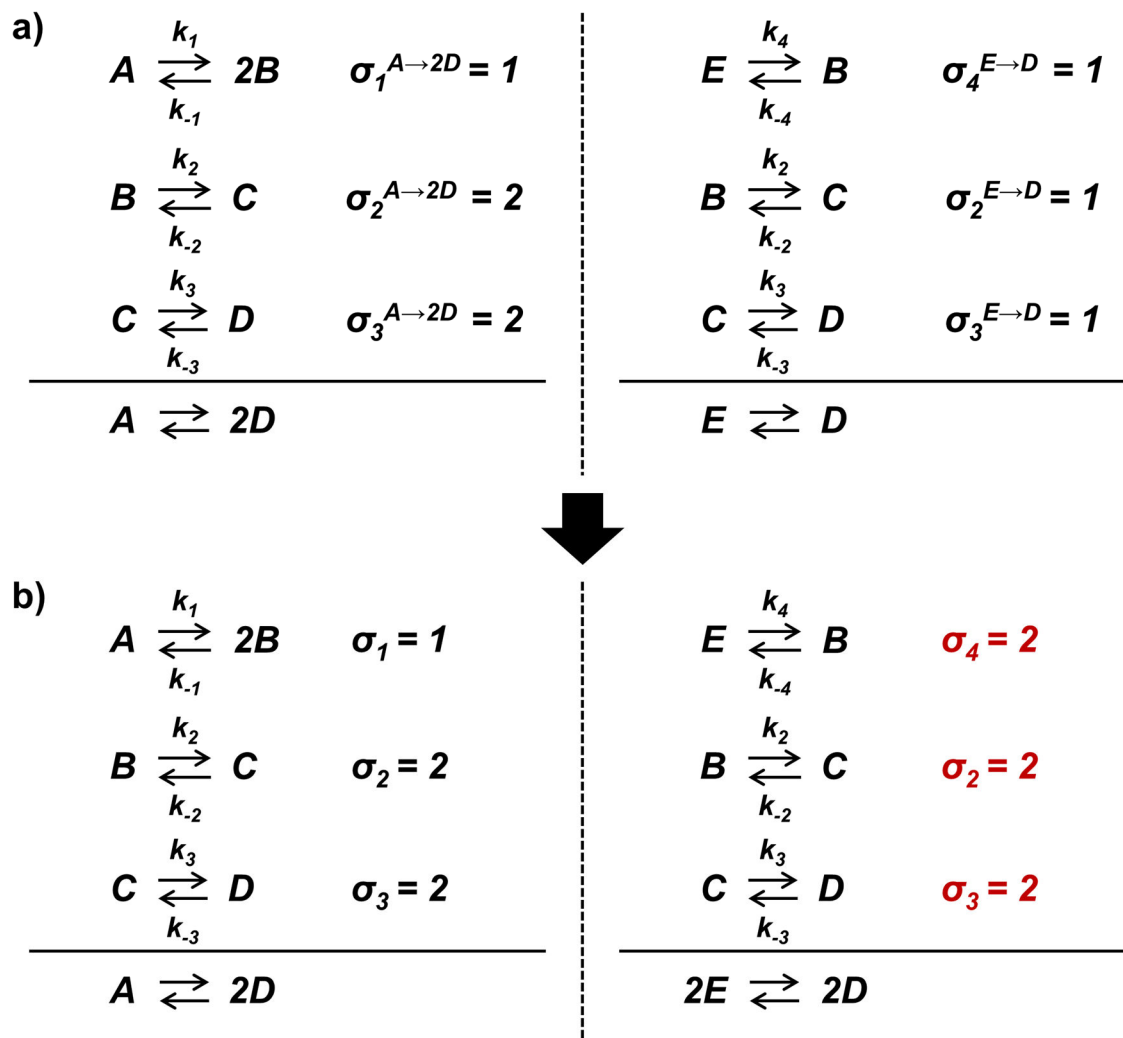
overall reactions with three elementary steps may occur (Scheme 4a). While the two overall reactions are distinct, the second and third elementary steps for each reaction are shared but have different stoichiometric numbers. The system as a whole constitutes an interconnected reaction network but the reaction network and land post diagram cannot be constructed yet due to the unequal stoichiometric numbers. In this scenario, we scale the overall reaction $E \rightleftharpoons D$ (right side of Scheme 4a) by a factor of two such that all stoichiometric numbers are consistent globally (Scheme 4b). By mass and atom balances, it is disallowed for the ratio between the stoichiometric numbers of shared elementary steps within one overall reaction to be different from that of another overall reaction; in other words, the scaling of overall reactions should always be able to resolve the unequal stoichiometric numbers. This then enables the combination of the two overall reactions into one interconnected reaction network and, consequently, the assignment of appropriate land posts (Fig. 9). The result again demonstrates the applicability of the formalisms outlined in the previous sections as long as the apparent elementary step unidirectional rates (\vec{r}'_i & \tilde{r}'_j) are used for any elementary step with non-unity stoichiometric number (Eq. 29).

$$\vec{r}'_i = \frac{\vec{r}_i}{\sigma_i} \quad (29a)$$

$$\tilde{r}'_i = \frac{\tilde{r}_i}{\sigma_i} \quad (29b)$$

The need to adjust both the forward and reverse unidirectional rates for elementary steps with non-unity stoichiometric numbers is congruent with the connectivity-independent nature of effective reversibility. Non-unity stoichiometric numbers will always cancel out when taking the ratio of apparent elementary step unidirectional rates such that the effective reversibility is independent of stoichiometric numbers and remains the product of the reversibilities of the elementary steps involved. Calculated unidirectional rates and effective reversibility for the reaction from A to 2D

in the system outlined in Scheme 4b reflect those obtained from simulation (Sec. S13; Fig. S10; SI). We next detail the requirements for rigorous isotopic tracing by considering systems with elementary steps involving multiple reactants and/or products.



Scheme 4. Example system with four unique elementary steps that constitute two overall reactions, each having three elementary steps, two of which are shared. (a) Conventional assignment of stoichiometric numbers for each reaction would lead to steps 2 and 3 having inconsistent stoichiometric numbers between the two reaction sequences. (b) Scaling of the overall reaction $E \rightleftharpoons D$ by two enables assignment of stoichiometric numbers that are consistent globally.

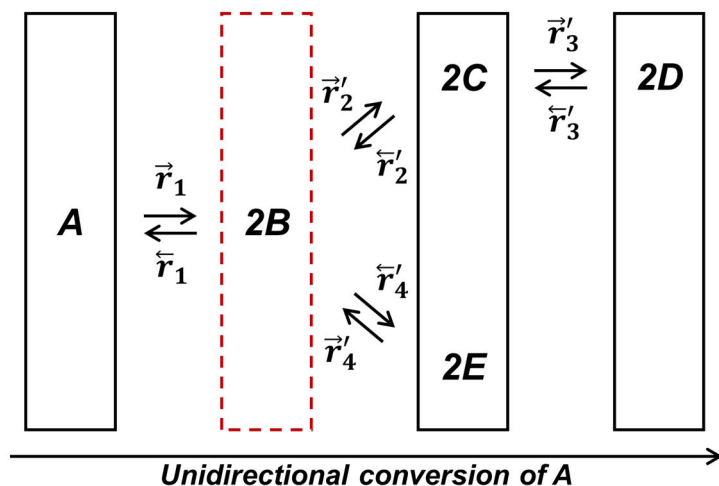
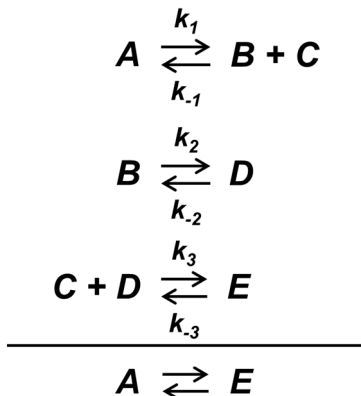


Figure 9. Rearrangement and land post assignment of the interconnected system shown in Scheme 4 for the unidirectional conversion of species A to 2D and 2E. The red-dashed land post signifies the nodal species after which the reaction network branches.

2.4 Limitations and requirements for rigorous isotopic tracing

While we have focused on cases with one reactant and product associated with each elementary step, rigorous isotopic tracing in systems with elementary steps involving multiple reactants and/or products requires each land post to contain a unique species. We first consider the system shown in Scheme 5 with the initial conditions of $C_{A,0} = 100$ a.u. and $C_{E,0} = 2$ a.u and the rate constants listed in Table S1. The associated land post diagram for the conversion of A to E (Fig. 10) is the same as that for the single-path system shown in Scheme 1. As the derivations detailed thus far have not specified the exact functional forms of the elementary step rates, the resulting expressions for unidirectional rates should remain valid. We hence rely again on simulated isotopic exchange rates to verify the validity of Equations 1 and 2; however, we here impose that isotopically-labeled A (A') only yield isotopically-labeled B (B') and does not yield isotopically-labeled C. Similarly, isotopically-labeled E (E') may only decompose to isotopically-labeled D (D') and unlabeled C. These constraints ensure no labeled C exists within the system, define rigorously what A' and E' are, and avoid the complexity where B'+C, B+C', and B'+C' each may form some kind of labeled A (and similarly for E with C+D). Indeed, Figure S11 (Sec.

S14; SI) demonstrates that the simulated isotopic exchange rates and effective reversibility reflect those calculated from Equations 1-3.



Scheme 5. Example reaction sequence with elementary steps involving multiple reactants and/or products for the formation of E from A with three reactive intermediates, species B, C, and D, that abide by the pseudo-steady-state assumption.

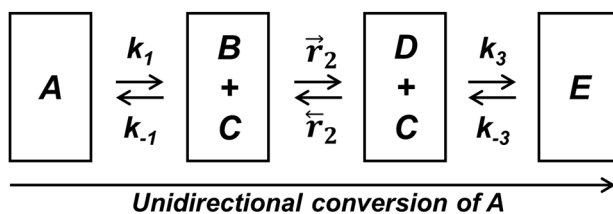
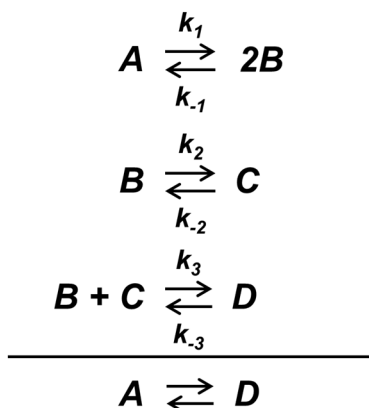


Figure 10. Land post assignment of the system shown in Scheme 5 for the unidirectional conversion of A to E. The second step is explicitly labeled with \vec{r}_2 and \vec{r}_2 as species C is not involved in the second elementary step.

We now consider another system shown in Scheme 6 that is similar to Scheme 5 except the first elementary step yields two B molecules. The key characteristic of this system is that there exists a land post (second one in this case) that lacks a unique species as species B, the sole reactant of the second elementary step, is also a reactant of the third elementary step (Fig. 11). This feature necessitates the definition of fully-labeled, partially-labeled, and unlabeled A and D as A can be formed from B+B, B'+B, B+B', or B'+B' while D can be formed from B+C, B'+C, B+C', or B'+C'. Despite the isotopic distribution of A and D following some fixed statistical distribution, the isotopic exchange rates will not be indicative of unidirectional rates as B exists in both the

second and third land posts. It is unclear exactly how the formation of partially-labeled D from B'+C or B+C' relates to the consumption of fully-labeled A. This complexity that arises for systems with land posts without unique species precludes a strict definition of isotopic exchange rates and, consequently, limits the use of isotopic exchange rates as tools to probe unidirectional rates.



Scheme 6. Example reaction sequence with elementary steps involving multiple reactants and/or products for the formation of D from A with two reactive intermediates, species B and C, that abide by the pseudo-steady-state assumption.

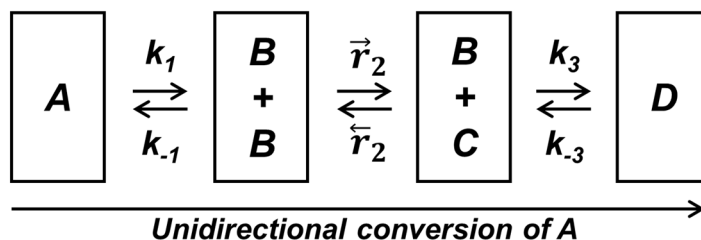


Figure 11. Land post assignment of the system shown in Scheme 6 for the unidirectional conversion of species A to species D. The second step is explicitly labeled with \vec{r}_2 and \vec{r}_2 as only one B is involved in the second elementary step.

In Scheme 4, the elementary step $A \rightleftharpoons 2B$ is also present but all land posts contain a unique species for the unidirectional forward and reverse rates from A to 2D (Fig. 9). When fully-labeled A and unlabeled D are fed, the formation of 2D' (from 2C') must correspond to the consumption of fully-labeled A. When unlabeled A and labeled D (D') are fed, we can form fully-labeled A (from B'+B') that corresponds to the consumption of 2D', partially-labeled A (from B+B' or B'+B)

that corresponds to the consumption of D', and unlabeled A (from B+B) that does not correspond to the consumption of D'. The fact that each land post retains a unique species still enables rigorous tracing of isotopes. The procedure for isotopic labeling of species in Scheme 5 also leveraged this characteristic to unambiguously define isotopic exchange rates. The utility of isotopic tracing is thus limited by the connectivity of the network rather than characteristics of individual elementary steps. Next, we expound further on the utility of effective reversibility for an interconnected reaction network from an experimental standpoint.

2.5 *Utility of reversibility in interconnected reaction networks*

The adherence of effective reversibility in an interconnected reaction network to the canonical definition of effective reversibility implies that all analyses based on reversibility, such as the De Donder relation and, more relevantly, the generalized de Donder relation, remain valid [2–4,12]. The subtlety for interconnected system arises when one attempts to extract information regarding the unidirectional rates based on net rates and effective reversibility. Given the net rate and the effective reversibility, the forward and reverse unidirectional rates can be calculated as

$$\vec{R} = R \left(\frac{1}{1 - Z_{\text{eff}}} \right) \quad (30a)$$

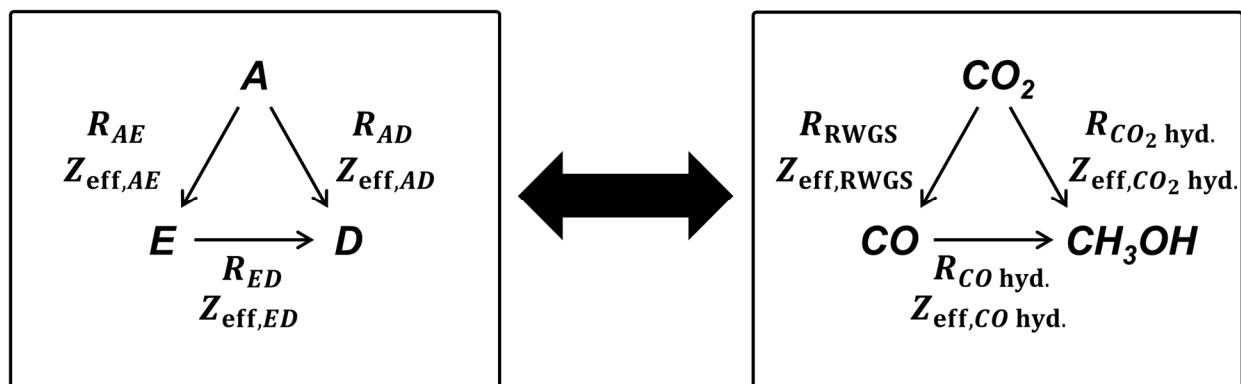
$$\tilde{R} = R \left(\frac{Z_{\text{eff}}}{1 - Z_{\text{eff}}} \right) \quad (30b)$$

where $R = \vec{R} - \tilde{R}$. While the net rate for a single-path system is equal to the net rate of generation of reactants and products after accounting for any stoichiometric coefficients, the same cannot be applied to an interconnected reaction network. Suppose we are to study the unidirectional rates within the reaction system shown in Scheme 2 without any knowledge of the connectivity between the stable species, the only quantities we can experimentally measure are the net rates of generation of the stable species (r_A , r_D , and r_E) along with the effective reversibilities between them ($Z_{\text{eff},AD}$,

$Z_{\text{eff},AE}$, and $Z_{\text{eff},ED}$), provided the stoichiometric numbers of all elementary steps are unity (Scheme 7). This is again analogous to the study of CO_x hydrogenation, where one can measure the net rates of generation of CO_2 , CH_3OH , and CO along with the effective reversibilities of CO_2 hydrogenation, RWGS, and CO hydrogenation. Any attempt to calculate the net rate of reaction between just two of the three stable species in order to invoke Equation 30 will be hindered by the fact that the system is underspecified (Eq. 31).

$$\begin{aligned} -R_{AD} - R_{AE} &= r_A \\ R_{AD} + R_{ED} &= r_D \\ R_{AE} - R_{ED} &= r_E \end{aligned} \Rightarrow \begin{bmatrix} -1 & -1 & 0 \\ 1 & 0 & 1 \\ 0 & 1 & -1 \end{bmatrix} \begin{bmatrix} R_{AD} \\ R_{AE} \\ R_{ED} \end{bmatrix} = \begin{bmatrix} r_A \\ r_D \\ r_E \end{bmatrix} \quad (31)$$

Thus, despite the path independence of effective reversibility, analyses of unidirectional rates for interconnected reaction networks pose innate difficulties that are not present in those for single-path reaction sequences. Conclusions regarding unidirectional rates, and even net rates between two stable species, must come from experiments such as isotopic tracing and exchange that provide additional information distinguishing rates of interconnected pathways. Unidirectional rates carry information regarding network connectivity and, as such, rigorous measurements and analyses of unidirectional forward and reverse rates may serve as evidence favoring or disproving certain proposed reaction mechanisms in addition to deconvoluting rates of co-occurring reaction pathways within an interconnected reaction network, each not conveyed by the effective reversibility alone.



Scheme 7. Generalized schematics of the reaction network in Scheme 2 as visualized without any information on the connectivity between stable species. Arrows indicate the presumed directions of reactions for which the net rates are defined to be positive. The analogous CO_x hydrogenation system is shown on the right with stoichiometric amounts of H_2 and H_2O neglected for simplicity.

3 Conclusion

Adopting the fundamental principle in the approach first set forth by Horiuti[1] to analyze unidirectional rates within single-path reaction networks, we show that the derivation can be generalized for complex interconnected reaction networks by accounting for branches in reaction pathways as alternative stable endpoints. Any addition and activation of elementary steps to alternative products impacts the functional forms of both the forward and reverse unidirectional rates with the inclusion of terms directly associated with the rates of the added steps but does so without changing the functional form of the effective reversibility. Expressions of unidirectional rates may be rationalized by noting that the kinetic resistance (inverse of unidirectional rate) is the sum of the single-path kinetic resistance of the elementary steps involved and the kinetic resistances contributed by the nodal species. The formalism presented in this work further applies to cases with non-unity stoichiometric numbers through the use of apparent elementary step unidirectional rates. We show that the calculated values of the unidirectional forward rate, unidirectional reverse rate, and, consequently, effective reversibility based on the derived functional forms agree with simulated isotopic exchange rates within an idealized PFR with enforced PSSH on reactive intermediates. The results outline the dichotomy between kinetic

properties such as reaction rates and thermodynamic quantities such as reversibility, where rates are connectivity-dependent while reversibility is not. As such, the canonical definition of effective reversibility (Eq. 3) applies to all reaction networks whereas the functional forms of the single-path unidirectional forward and reverse rates shown by Horiuti[1] and Temkin[16–18] should strictly be used for single-path reaction systems. The presence of nodes in a reaction network prevents the calculation of unidirectional rates based on the net rates of generation of stable species and the effective reversibility alone; however, unidirectional rates, as measured with isotopic tracers given that each elementary step of the overall reaction and each land post involves a unique species, can be used to validate proposed reaction network connectivity for such systems. As the catalysis and reaction kinetics community continues to investigate and explicate rates and mechanisms of increasingly complex systems, this study aims to provide the mathematical basis for the formulation of rates and reversibility beyond the base case of single-path reaction networks.

4 Supporting Information

Derivation of single-path unidirectional rates following Horiuti’s formalism and Temkin’s product rule, computational code for the simulation of isotopic exchange rates, simulated isotopic exchange rates for model interconnected networks, derivations of unidirectional rates, effective reversibilities, and kinetic resistances for model interconnected networks, analogy of nodal resistances in electrical circuits

5 Acknowledgements

This work was supported by the US Department of Energy, Office of Basic Energy Science, Catalysis Science Program (Award DE-SC00019028). Additional financial support was received from the National Science Foundation Graduate Research Fellowship and the University of Minnesota College of Science and Engineering Graduate Fellowship.

6 References

- [1] J. Horiuti, Unidirectional rates of reaction of single route, *J. Res. Inst. Catal. Hokkaido Univ.* 20 (1972) 225–228.
- [2] N.K. Razdan, A. Kumar, B.L. Foley, A. Bhan, Influence of ethylene and acetylene on the rate and reversibility of methane dehydroaromatization on Mo/H-ZSM-5 catalysts, *J. Catal.* 381 (2020) 261–270. doi:10.1016/j.jcat.2019.11.004.
- [3] B.L. Foley, A. Bhan, Degree of rate control and De Donder relations – An interpretation based on transition state theory, *J. Catal.* 384 (2020) 231–251. doi:10.1016/j.jcat.2020.02.008.
- [4] B.L. Foley, A. Bhan, Thermodynamically consistent forward and reverse degrees of rate control in reversible reactions, *J. Catal.* 389 (2020) 566–577. doi:10.1016/j.jcat.2020.06.013.
- [5] J. Sehested, Industrial and scientific directions of methanol catalyst development, *J. Catal.* 371 (2019) 368–375. doi:10.1016/j.jcat.2019.02.002.
- [6] L.C. Grabow, M. Mavrikakis, Mechanism of methanol synthesis on Cu through CO₂ and CO hydrogenation, *ACS Catal.* 1 (2011) 365–384. doi:10.1021/cs200055d.
- [7] R. Gaikwad, H. Reymond, N. Phongprueksathat, P. Rudolf von Rohr, A. Urakawa, From CO or CO₂?: Space-resolved insights into high-pressure CO₂ hydrogenation to methanol over Cu/ZnO/Al₂O₃, *Catal. Sci. Technol.* 10 (2020) 2763–2768. doi:10.1039/D0CY00050G.
- [8] J.S. Yoo, F. Abild-Pedersen, J.K. Nørskov, F. Studt, Theoretical analysis of transition-metal catalysts for formic acid decomposition, *ACS Catal.* 4 (2014) 1226–1233. doi:10.1021/cs400664z.
- [9] J.A. Herron, J. Scaranto, P. Ferrin, S. Li, M. Mavrikakis, Trends in formic acid decomposition on model transition metal surfaces: A density functional theory study, *ACS Catal.* 4 (2014) 4434–4445. doi:10.1021/cs500737p.
- [10] A. Hwang, A. Bhan, Bifunctional strategy coupling Y₂O₃-catalyzed alkanal decomposition with methanol-to-olefins catalysis for enhanced lifetime, *ACS Catal.* 7 (2017) 4417–4422. doi:10.1021/acscatal.7b00894.
- [11] P.B. Weisz, Polyfunctional heterogeneous catalysis, in: *Adv. Catal.*, 1962: pp. 137–190. doi:10.1016/S0360-0564(08)60287-4.
- [12] M. Boudart, Thermodynamic and kinetic coupling of chain and catalytic reactions, *J. Phys. Chem.* 87 (1983) 2786–2789. doi:10.1021/j100238a018.
- [13] M. Boudart, G. Djega-Mariadassou, Kinetic coupling in and between catalytic cycles, *Catal. Letters.* 29 (1994) 7–13. doi:10.1007/BF00814246.
- [14] A. Matsuda, J. Horiuti, The relation between stoichiometric number and exchange reaction, *J. Res. Inst. Catal. Hokkaido Univ.* 10 (1962) 14–23. <http://hdl.handle.net/2115/24752>.

- [15] C. Bokhoven, M.J. Gorgels, P. Mars, Stoichiometric number and reaction mechanism of the ammonia synthesis, *Trans. Faraday Soc.* 55 (1959) 315. doi:10.1039/tf9595500315.
- [16] J. Horiuti, Theory of reaction rates as based on the stoichiometric number concept, *Ann. N. Y. Acad. Sci.* 213 (1973) 5–30. doi:10.1111/j.1749-6632.1973.tb51052.x.
- [17] M. Boudart, Some applications of the generalized De Donder equation to industrial reactions, *Ind. Eng. Chem. Fundam.* 25 (1986) 70–75. doi:10.1021/i100021a010.
- [18] M.I. Temkin, The kinetics of some industrial heterogeneous catalytic reactions, in: *Adv. Catal.*, 1979: pp. 173–291. doi:10.1016/S0360-0564(08)60135-2.
- [19] J.A. Dumesic, Analyses of reaction schemes using De Donder relations, *J. Catal.* 185 (1999) 496–505. doi:10.1006/jcat.1999.2523.
- [20] I. Fishtik, C.A. Callaghan, R. Datta, Reaction route graphs. I. Theory and algorithm, *J. Phys. Chem. B.* 108 (2004) 5671–5682. doi:10.1021/jp0374004.
- [21] J.A. Dumesic, Reply to finding the rate-determining step in a mechanism: Comparing DeDonder relations with the “degree of rate control,” *J. Catal.* 204 (2001) 525–529. doi:10.1006/jcat.2001.3397.

TOC Graphic:

